Electronic Supplementary Material (ESI) for Catalysis Science & Technology.

Influence of Re-M interaction in Re-M/C bimetallic catalysts prepared by microwave-assisted thermolytic method on aqueous-phase hydrogenation of succinic acid

Xin Di [a], Chuang Li [a], Gwendoline Lafaye [b,] *, Especel Catherine [b], Epron Florence[b],
Changhai Liang [a,] *

[a] Laboratory of Advanced Materials and Catalytic Engineering, Dalian University of Technology, Dalian 116024, P.R. China.

[b] Institut de Chimie, des Milieux & Matériaux (IC2MP), Université de Poitiers, Poitiers 86073, France.

* Corresponding author. Tel: +86-0411-84986353; Fax: +86-0411-84986353; E-mail: changhai@dlut.edu.cn, gwendoline.lafaye@univ-poitiers.fr

1. Catalysts preparation

The scheme of microwave-assistant thermolytic method

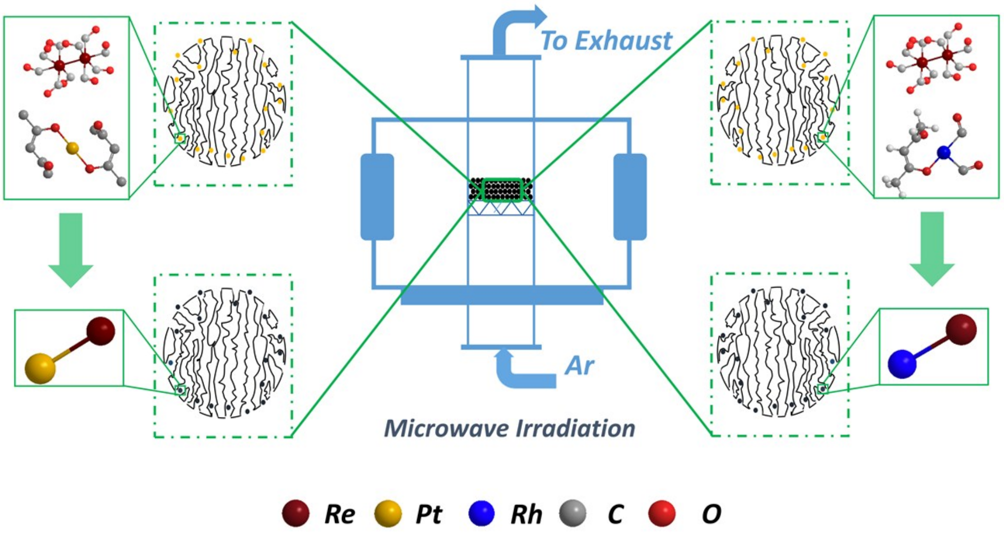

2. Characterization method

The metallic loading of monometallic and bimetallic catalysts were analyzed by inductively coupled plasma atomic emission spectroscopy equipment (ICP-AES, Optima 2000DV, PerkinElmer, USA) after dissolution of the catalysts.

CO chemisorption was measured with Autosorb-iQ (Quantachrome, USA) equipment to estimate metal dispersion of the monometallic and Re-M/C bimetallic catalysts. Prior to CO chemisorption, the samples were reduced in situ under hydrogen atmosphere for 100 min at 300°C for Rh/C and Re-Rh/C, at 400°C for Re/C and Re-Pt/C and at 350°C for Pt/C, and then evacuated under high vacuum for 120 min. The CO chemisorption experiments were performed at 30°C. The amount of irreversibly adsorbed CO was determined as the extrapolation of the difference between the total uptake and the reversible uptake to zero pressure.

Powder X-ray diffraction (XRD) of the catalysts was used to probe metallic interaction and to provide information regarding crystal phase. Powder diffraction was performed by Rigaku XRD diffraction meter (Rigaku D/Max-RB, Rigaku, Japan) using CuKα (λ=1.54178 Å) as the radiation source, operated at 40 kV and 100 mA with a scan speed of 8 ° min^{-1}.

Temperature-programmed reduction (TPR) analyses were performed on an AutoChem 2910 instrument (Quantachrome, USA) equipped with a thermal conductivity detector (TCD). Prior to the TPR analysis, the samples were firstly treated with inert gas for 1 h at 200°C, and cooled down to ambient temperature. The atmosphere were then changed to 10% H_2/Ar and kept for 40 min. This treating procedure was then followed by a TPR analysis using 10% H_2/Ar at a flow rate of 100 mL min^{-1} from room temperature to 800 °C with a temperature ramping rate of 10 °C min^{-1}.

Temperature-programmed desorption (TPD) was carried out to study the ability of hydrogen adsorption and activation on Re-M/C bimetallic catalysts. The Re-M/C catalysts were loaded into the fritted quartz tube, pretreated at 300°C for Re-Rh/C and at 400°C for Re-Pt/C during 100 min under 10% H_2/Ar atmosphere and afterwards cooled down to 50°C under N_2 atmosphere. H_2 adsorption was performed at 50°C in 10% H_2/Ar mixture with a flow rate of 100 mL (STP)/min. After H_2 adsorption, the samples were purged with N_2 for 120 min. The H_2 desorption was then detected under N_2 atmosphere with a temperature ramp of 5 °C min^{-1} from 50 to 900°C.

X-ray photoelectron spectroscopy (XPS) measurements were performed on an ESCALAB250 instrument (Thermo VG, USA). Monochromatic AlKα source (hν = 1486.6 eV) was used at a power of 150 W. The survey scans were collected for binding energy spanning from 800 to 0 eV. The pass energy was 50 eV with a step of 0.1 eV for high-resolution spectra. In the test, binding energies were referenced to C 1s (284.6 eV).

Before the XPS measurements, the samples were pre-reduced in tube furnace at the same time and then cooled down to room temperature under Ar. Air was slowly pumped into the tube furnace after reduction to avoid the intense oxidation of catalysts. After that, the catalysts were stored in sample bottles under ambient atmosphere for the same period of time. At the end, these samples were analyzed by XPS simultaneously, in order to increase the accuracy of results.

Transmission electron microscopy (TEM) images were performed on a FEI Technai F20 electron microscope. The HAADF-STEM and corresponding elemental mapping were performed in STEM mode in combination with energy dispersive X-ray spectroscopy (EDX) using a DX4 analyzer system (EDAX). The reduced catalysts were dispersed in ethanol with ultrasound. The average diameters were calculated by measuring over 200 particles from various TEM images.

3. Cyclohexane Dehydrogenation

The cyclohexane dehydrogenation reaction was performed in a fixed-bed reactor at atmospheric pressure. A mass of 0.02 g of catalysts were reduced at 300°C for Rh/C and Re-Rh/C, at 400°C for Re/C and Re-Pt/C and at 350°C for Pt/C, for 120 min and the temperature was decreased to 260°C for reaction. Cyclohexane was injected using a calibrated motor-driven syringe (0.03 mL/min) in a hydrogen flow (100 mL/min). The products were analyzed for every 10 minutes by GC and the only detected product was benzene.

4. Kinetic Study

4.1 Assessing transport control in aqueous hydrogenation of SA

Since the reaction occurred in a heterogeneous system (liquid-gas-solid), it is essential to consider the influence of external and internal transport for kinetic study in this experiment.

4.1.1 The influence of external diffusion

Given the uncertainty in estimating mass transfer coefficients, experimental analysis of external mass transport limitations is reasonable. For autoclave reactor, increasing stirring speed not only contributes to the mass transfer of SA, but also is benefit to the diffusion of H_2 in aqueous solutions. Thus the hydrogenation of SA was carried out over different stirring speeds (from 300 to 900 rpm) while maintaining constant the other reaction parameters. A small increase in hydrogenation rate was observed by increasing stirring rate when the stirring speed was above 700 rpm. These results reveal that external transfer of SA and H_2 is sufficiently rapid since the influence on the rate of hydrogenation is limited. Therefore, 800 rpm was sufficient in this system to eliminate external diffusion effect as much as possible.

4.1.2 The influence of internal diffusion

The Thiele Modulus (φ) in the equation below is often used to estimate the influence of internal diffusion on the reaction rate.

$$\varphi = \frac{V_p}{a_p}\sqrt{\frac{k_v}{D_e}}$$

Here, V_p is the volume of catalyst, a_p is the exterior surface area of catalyst, k_v is the reaction rate constant based on the volume of catalyst, D_e is the effective diffusion coefficient. In this experiment, the TOFs over Re-Pt/C bimetallic catalysts with different particle sizes (< 75 μm, 75-100 μm and 100-150 μm) for SA hydrogenation were measured when the reaction rate was sufficiently high (i.e.: at 220°C) and then when the internal diffusion is likely to control the reaction rate. The results showed that the TOFs exhibit slight fluctuations for these three particle sizes, showing that the internal diffusion did not significantly control the reaction rate when the particle size was below 150 μm. The Thiele Modulus (φ) was small enough for any reasonable effective diffusion coefficient when the particle size was less than 100 μm, suggesting the influence of internal diffusion could be ignored. Thus, all catalysts in this study were sieved to make sure that the particle size is less than 75 μm.

4.2 The fitting method

The reaction order of SA concentration: the reaction order was fitted from the slope of double logarithmic plot for initial reaction rate vs initial SA concentration. (1) The reaction rate constant (*k*) for each data point at the specific reaction time and concentration was calculated assuming a zero reaction order. (2) The initial reaction rate (*r*) was calculated according to the reaction rate constant from step 1, and then the new reaction order was obtained according to the slope of double logarithmic plot. (3) The calculations of (1) and (2) were repeated until the reaction order converged. The number of iterations was usually less than three times.

The reaction order of H_2 pressure: according to the reaction order of SA concentration, the reaction rate constants for different H_2 pressure were calculated with the time course of SA hydrogenation by using Matlab or Origin. The reaction order of H_2 pressure was fitted from the slope of double logarithmic plot for reaction rate constant vs H_2 pressure. The degree of correlation will examine the above fitting results.

The apparent activation energy: according to the reaction order of SA concentration, the reaction rate constants under different temperatures were calculated with the time course of SA hydrogenation by using Matlab or Origin. After that, apparent activation energy was calculated on the basis of reaction rate constants with Origin and the degree of correlation will examine the above fitting results.

The reaction orders and apparent activation energy for GBL hydrogenation were calculated with the same method as provided above.

Tables and Figures

Table S1. The TOFs for the dehydrogenation of cyclohexane over Re/C, M/C and Re-M/C catalysts (M = Pt or Rh).

Catalysts	Experimental TOFs (min^{-1})	Calculated TOFs (min^{-1})
Pt/C	154	—
Re-Pt/C	87	82
Re/C	9.5	—
Re-Rh/C	20	16
Rh/C	22	—

Reaction conditions: atmospheric pressure, 260 °C, 0.02 g of catalysts

Table S2. XPS analyses results of Re/C, M/C and Re-M/C catalysts (M = Pt or Rh).

Catalysts	Re 4f (%)			Pt 4f (%)			Rh 3d (%)
	Re^0	Re^{4+}	Re^{6+}	Pt^0	Pt^{2+}	Pt^{4+}	Rh^0
Pt/C				52	32	16	
Re-Pt/C	38	12	50	40	48	12	
Re/C	10	17	73				
Re-Rh/C	16	19	65				—
Rh/C							100

Table S3. H_2-TPD analyses results of Re/C, M/C and Re-M/C catalysts (M = Pt or Rh).

Catalysts	Relative desorption quantity		
	Peak I	Peak II	Total
Pt/C	1.0	1.6	2.6
Re-Pt/C	0.8	2.5	3.3
Re/C	1.3	1.0	2.3
Re-Rh/C	0.7	1.9	2.6
Rh/C	0.3	1.1	1.4

Table S4. Hydrogenation of intermediates over Re-M/C bimetallic catalysts (M = Pt or Rh).

Substrate	Catalysts	Con.(%)	Sel.(%)						
			GBL	BDO	THF	NBA	NPA	BA	PA
GBL	Re-Pt/C	48.4	—	36.1	59.6	2.7	1.8		
	Re-Rh/C	60.0	—	47.0	30.8	3.9	18.3		
BDO	Re-Pt/C	23.1	9.7	—	86.0	3.0	1.3		
	Re-Rh/C	32.7	10.2	—	34.2	12.3	43.3		
THF	Re-Pt/C	5.6			—		100		
	Re-Rh/C	1.1			—		100		
PA	Re-Pt/C	75.5					100		—
	Re-Rh/C	74.3					100		—
BA	Re-Pt/C	78.1				100		—	
	Re-Rh/C	67.8				100		—	

Reaction conditions: 220°C, 8.0 MPa, 0.1 g of catalyst, Re-Rh/C: 2 h, Re-Pt/C: 6 h.

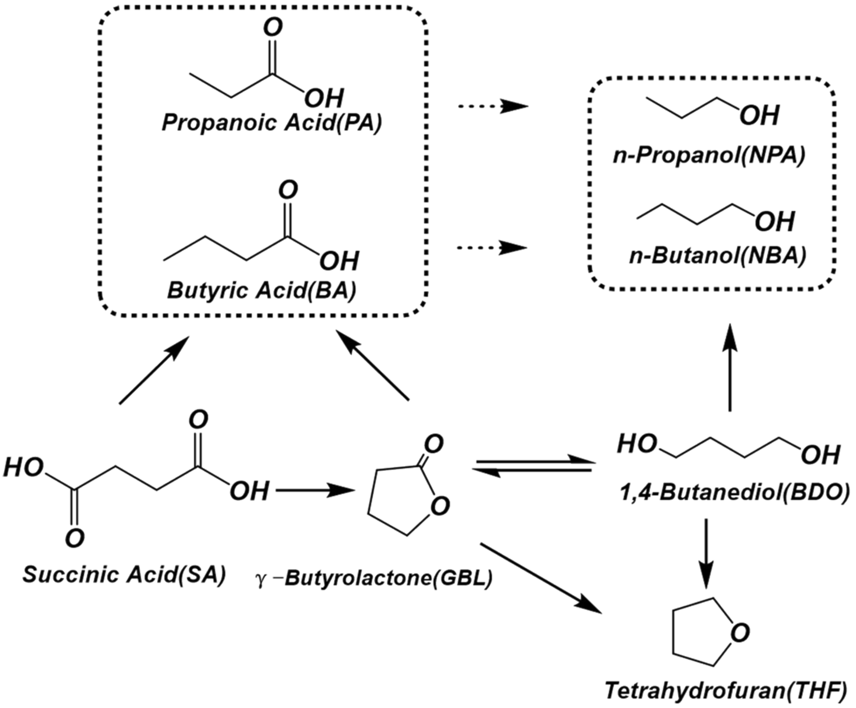

Scheme S1. The main reactive routes for the catalytic hydrogenation of succinic acid.

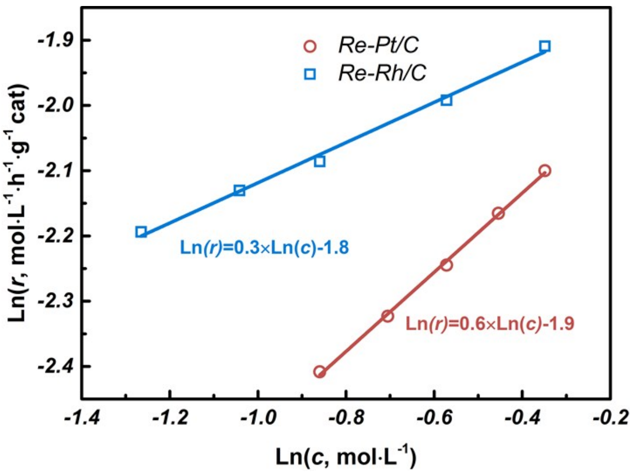

Fig. S1. Effect of initial SA concentration in the hydrogenation of SA over Re−Pt/C and Re-Rh/C. (the correlation coefficient R^2 for each catalyst is above 0.99). Reaction conditions: 200°C, 8.0 MPa, 0.2 g of catalyst for Re-Pt/C, 0.1 g of catalyst for Re-Rh/C.

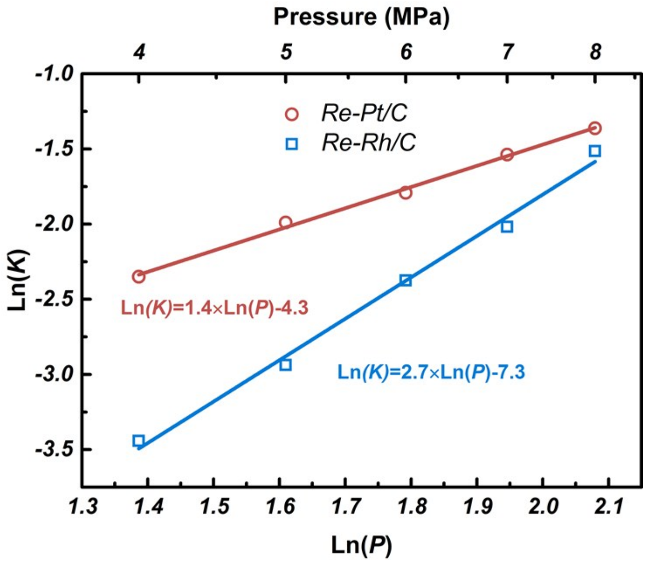

Fig. S2. The dependence of reaction rate constant (*k*) on hydrogen pressure during the hydrogenation of SA over Re-Pt/C and Re-Rh/C catalysts (the correlation coefficient R^2 for each catalyst is above 0.99). Reaction conditions: 220°C, 0.1 g of catalyst for Re-Pt/C and Re-Rh/C.

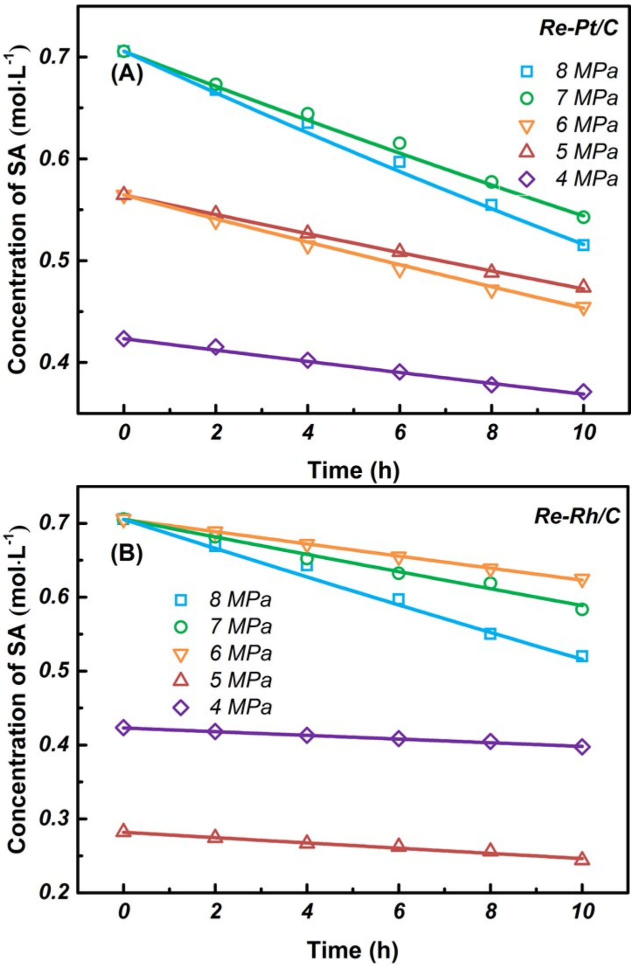

Fig. S3. Time course of SA hydrogenation at different pressure over Re-Pt/C (A) and Re-Rh/C (B) (the correlation coefficient R^2 for each catalyst at different pressure is above 0.99). The plot is raw data and the solid line is fitting result. Reaction conditions: 220°C, 0.1 g of catalyst for Re-Pt/C and Re-Rh/C.

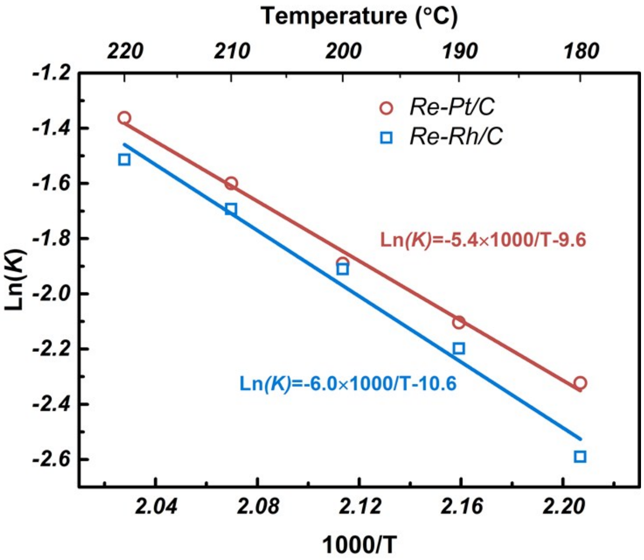

Fig. S4. Arrhenius plots for the hydrogenation of SA to GBL over Re-Pt/C and Re-Rh/C catalysts (the correlation coefficient R^2 for Re-Pt/C and Re-Rh/C is above 0.98). Reaction conditions: 8 MPa, 0.1 g of catalyst for Re-Pt/C and Re-Rh/C.

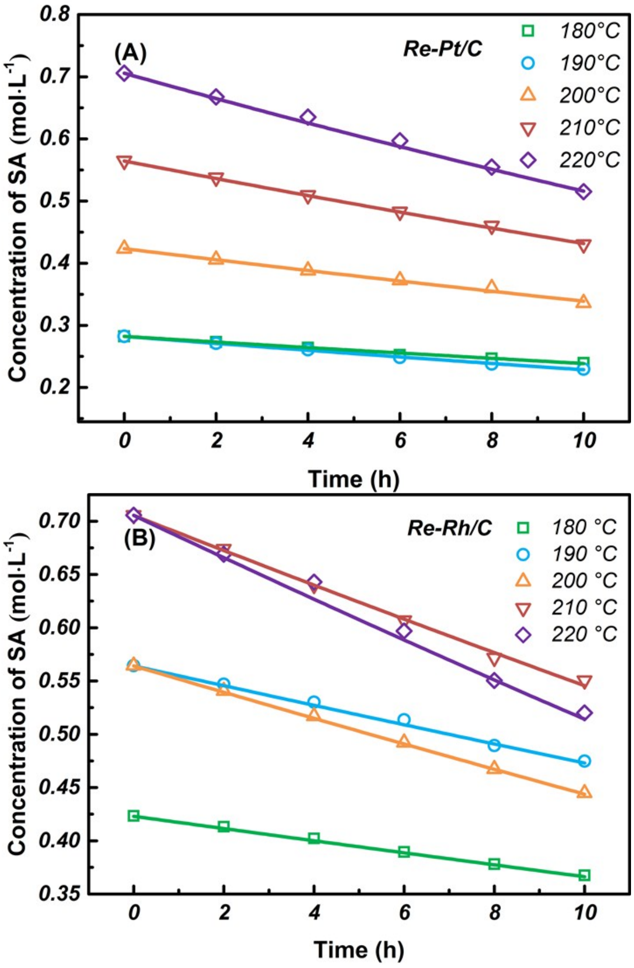

Fig. S5. Time course of SA hydrogenation at different temperature over Re-Pt/C (A) and Re-Rh/C (B) (the correlation coefficient R^2 for each catalyst at different temperature is above 0.99). The plot is raw data and the solid line is fitting result. Reaction conditions: 8 MPa, 0.1 g of catalyst for Re-Pt/C and Re-Rh/C.

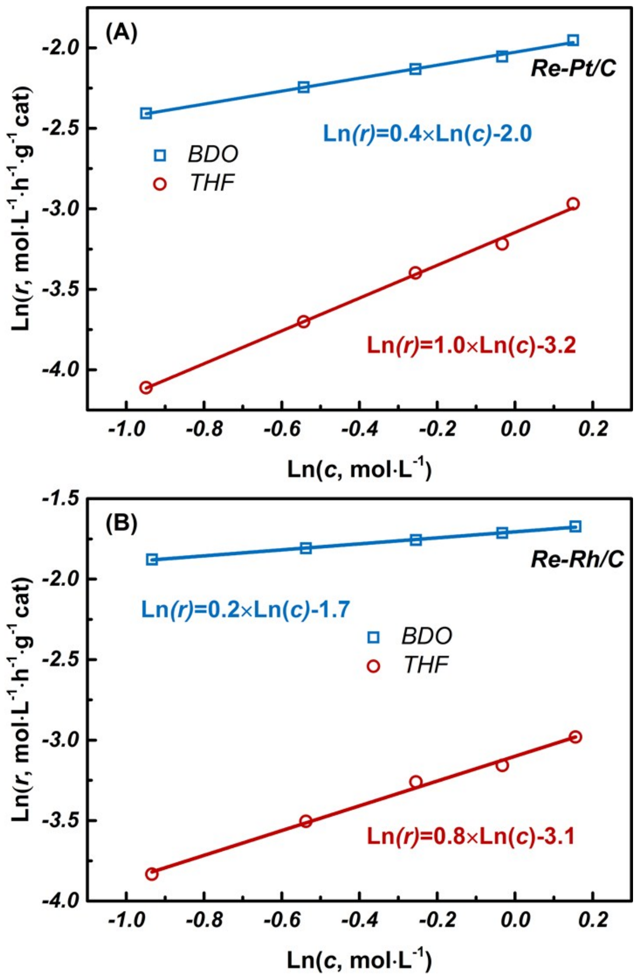

Fig. S6. Effect of initial GBL concentration in the hydrogenation of GBL over Re−Pt/C (A) and Re-Rh/C (B) (the correlation coefficient R^2 for each catalyst is above 0.99). Reaction conditions: 180°C, 8.0 MPa, 0.2 g of catalyst for Re-Pt/C and Re-Rh/C.

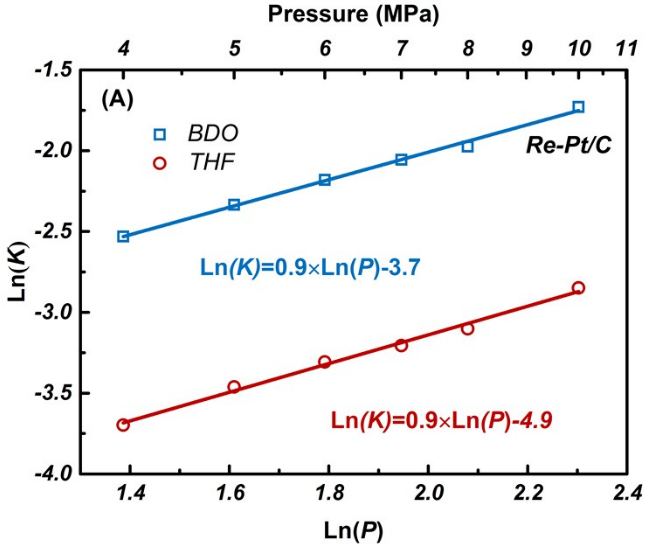

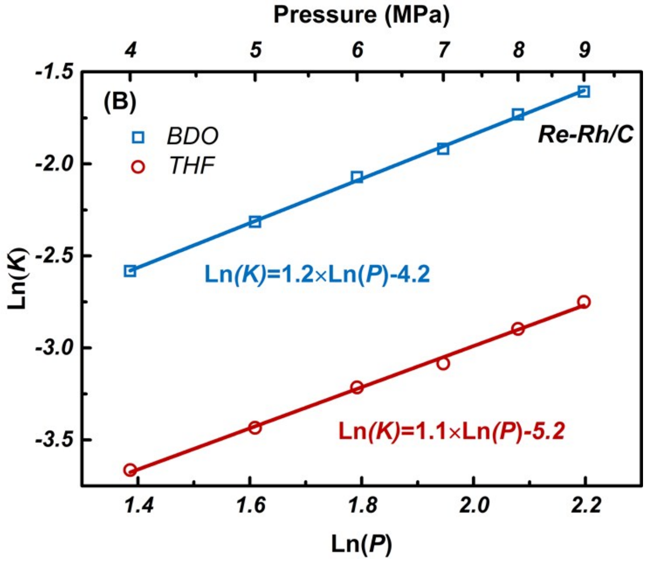

Fig. S7. The dependence of reaction rate constants (*k*) on hydrogen pressure for the hydrogenation of GBL over Re-Pt/C (A) and Re-Rh/C catalysts (B) (the correlation coefficient R^2 for each catalyst is above 0.99). Reaction conditions: 180 °C, 0.2 g of catalyst for Re-Pt/C and Re-Rh/C.

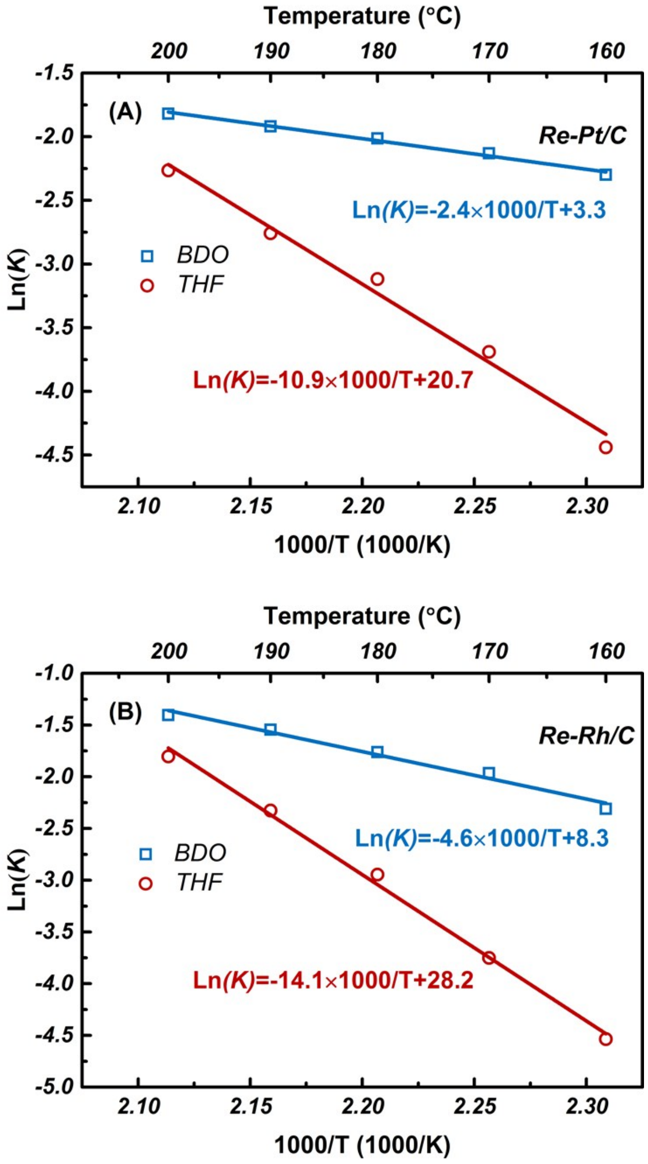

Fig. S8. Arrhenius plots for the hydrogenation of GBL to THF and BDO over Re-Pt/C (A) and Re-Rh/C (B) catalysts (the correlation coefficient for each catalyst $R^2>0.98$). Reaction conditions: 8 MPa, 0.2 g of catalyst for Re-Pt/C and Re-Rh/C.

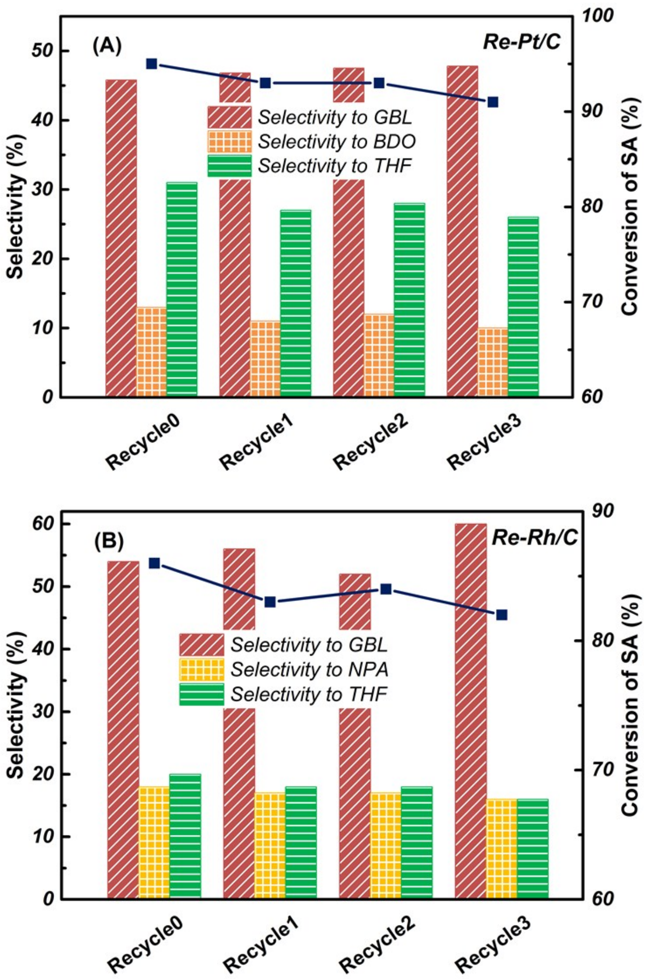

Fig. S9. Aqueous hydrogenation of succinic acid over Re-Pt/C (A) and Re-Rh/C (B) catalysts with respect to recycle run. Reaction conditions: 220 °C, initial pressure 8.0 MPa, 20 g solution (5 wt.% SA), 0.2 g catalyst, 4 h.